Synthetic and Systems Biotechnology 8 (2023) 486–497

Contents lists available at ScienceDirect

Synthetic and Systems Biotechnology

journal homepage: www.keaipublishing.com/en/journals/synthetic-and-systems-biotechnology

Original Research Article

Enhancing tylosin production by combinatorial overexpression of efflux, SAM biosynthesis, and regulatory genes in hyperproducing *Streptomyces xinghaiensis* strain

Penghui Dai [a], Yuyao Qin [a], Luyuan Li [b], Haidi Li [c], Lihuo Lv [c], Danying Xu [c], Yuqing Song [c], Tingting Huang [a], Shuangjun Lin [a,d], Zixin Deng [a,d], Meifeng Tao [a,d,*]

[a] State Key Laboratory of Microbial Metabolism, School of Life Sciences and Biotechnology, Shanghai Jiao Tong University, Shanghai, 200240, China
[b] Zhejiang Apeloa Biotechnology Co., Ltd., Jinhua, 322109, China
[c] Zhejiang Apeloa Jiayuan Pharmaceutical Co., Ltd., Jinhua, 322118, China
[d] Haihe Laboratory of Synthetic Biology, Tianjin, 300308, China

ARTICLE INFO

Keywords:
Streptomyces xinghaiensis
Tylosin
Combinational metabolic engineering

ABSTRACT

Tylosin is a 16-membered macrolide antibiotic widely used in veterinary medicine to control infections caused by Gram-positive pathogens and mycoplasmas. To improve the fermentation titer of tylosin in the hyperproducing *Streptomyces xinghaiensis* strain TL01, we sequenced its whole genome and identified the biosynthetic gene cluster therein. Overexpression of the tylosin efflux gene *tlrC*, the **c**luster-**s**ituated *S*-adenosyl methionine (SAM) synthetase gene $metK_{cs}$, the SAM biosynthetic genes $adoK_{cs}$-$metF_{cs}$, or the pathway-specific activator gene *tylR* enhanced tylosin production by 18%, 12%, 11%, and 11% in the respective engineered strains TLPH08-2, TLPH09, TLPH10, and TLPH12. Co-overexpression of $metK_{cs}$ and $adoK_{cs}$-$metF_{cs}$ as two transcripts increased tylosin production by 22% in the resultant strain TLPH11 compared to that in TL01. Furthermore, combinational overexpression of *tlrC*, $metK_{cs}$, $adoK_{cs}$-$metF_{cs}$, and *tylR* as four transcripts increased tylosin production by 23% (10.93g/L) in the resultant strain TLPH17 compared to that in TL01. However, a negligible additive effect was displayed upon combinational overexpression in TLPH17 as suggested by the limited increment of fermentation titer compared to that in TLPH08-2. Transcription analyses indicated that the expression of *tlrC* and three SAM biosynthetic genes in TLPH17 was considerably lower than that of TLPH08-2 and TLPH11. Based on this observation, the five genes were rearranged into one or two operons to coordinate their overexpression, yielding two engineered strains TLPH23 and TLPH24, and leading to further enhancement of tylosin production over TLPH17. In particular, the production of TLPH23 reached 11.35 g/L. These findings indicated that the combinatorial strategy is a promising approach for enhancing tylosin production in high-yielding industrial strains.

1. Introduction

Macrolides are antibiotics of choice for treating many common bacterial diseases in humans and animals, such as gastroenteritis and respiratory infections. Tylosin is a 16-membered macrolide widely used in veterinary medicine to control infections caused by Gram-positive organisms, mycoplasmas, and *Campylobacter*, owing to its broad-spectrum, safety, and oral efficacy [1]. Tylosin is also the critical substrate for the synthesis of third-generation macrolides such as tylvalosin, tilmicosin, and tildipirosin [2,3].

Tylosin was isolated from the fermentation broth of *Streptomyces fradiae* [4], *S. hygroscopicus* [5], and *S. rimosus* [6], among which *S. fradiae* (also named *S. xinghaiensis*) is used in industrial production [7,8]. Structurally, tylosin is composed of a 16-membered macrolactone ring and three deoxyhexose sugars (mycaminose, mycarose, and mycinose). The tylosin biosynthetic gene cluster of *S. fradiae* has been elucidated, which contains at least 43 open reading frames (ORFs) involved in assembly and modification of the macrolactone skeleton, biosynthesis and attachment of the deoxyhexose sugar moieties, self-resistance, transportation, regulation, and unknown function

Peer review under responsibility of KeAi Communications Co., Ltd.
* Corresponding author. State Key Laboratory of Microbial Metabolism, School of Life Sciences and Biotechnology, Shanghai Jiao Tong University, Shanghai, 200240, China.
E-mail address: tao_meifeng@sjtu.edu.cn (M. Tao).

https://doi.org/10.1016/j.synbio.2023.07.002
Received 24 April 2023; Received in revised form 29 June 2023; Accepted 6 July 2023
Available online 7 July 2023

[9–11]. The production of tylosin in *S. fradiae* is regulated by five cluster-situated regulatory genes encoding two repressors (TylP and TylQ) and three activators (TylS, TylU, and TylR) via a complex cascade. TylP is a deduced gamma-butyrolactone receptor that downregulates *tylP*, *tylQ*, and *tylS* by targeting their promoters. TylR is a pathway-specific activator that directly activates transcription of tylosin biosynthetic genes, and the expression of *tylR* is controlled by the activators (TylS and TylU) and the repressor TylQ [11–13].

Industrial production of antibiotics requires strain improvement to reduce manufacturing costs. Random mutagenesis [14,15], medium optimization [16,17], and genome shuffling [18] were practically utilized for strain improvement for tylosin production; however, these approaches relied on empirical screening and are time-consuming. Rational metabolic engineering strategies are effective in enhancing the yield of macrolide antibiotics, such as enhancing the supply of biosynthetic precursors or cofactors [19], overexpressing efflux or resistance genes [20], and manipulating the regulation of biosynthetic pathways [21]. Inactivation of the repressor genes, *tylP* or *tylQ*, has been found to be responsible for elevated tylosin production in mutants obtained via random mutagenesis breeding [22–24]. Overexpression of cluster-situated activator genes *tylR* and *tylS* has been demonstrated to increase production of tylosin [12,25]. Additionally, the yield of many macrolides, such as pikromycin [26], salinomycin [27], ascomycin [28], pristinamycin [29], and avermectin [30], was effectively enhanced by the combination of multiple metabolic engineering strategies. In a recent study, a genomics-based combinatorial engineering strategy was established in *Actinoplanes deccanensis*, resulting in improvement in fidaxomicin production (27-fold, 619.2 mg/L) and the genetic stability of the producing strain [31].

In the present study, we aimed to enhance the extracellular production of tylosin in an industrial producer, *S. xinghaiensis* TL01, using a combinatorial metabolic engineering strategy. We sequenced the whole genome of TL01 and identified the tylosin biosynthetic gene cluster. Single overexpression of the tylosin efflux gene, *S*-adenosyl methionine (SAM) biosynthetic genes, or the pathway-specific activator gene *tylR* resulted in significant enhancement of extracellular tylosin production. These genes were combined for co-overexpression, which led to a slight additional improvement in tylosin production. To solve this problem, we performed transcriptome analysis on the engineered strains and developed a fine-tuned combinatorial approach that led to further elevation of tylosin production. These observations provided valuable guidance for enhancing the production of other critical secondary metabolites in the high-yielding strains.

2. Materials and methods

2.1. Bacterial strains, plasmids, primers, and culture conditions

The bacterial strains and plasmids used in this study are listed in Table S1, and the primers are listed in Table S2. *S. xinghaiensis* TL01, which is an empirically improved strain used for industrial production of tylosin, was used as the starting strain for improving production. *S. xinghaiensis* strains were grown on 2CM plates (1.0% soluble starch, 0.2% tryptone, 0.1% NaCl, 0.2% $(NH4)_2SO_4$, 0.1% K_2HPO_4, 0.1% $MgSO_4$, 0.2% $CaCO_3$, 1.2% agar, and 1.0 mL inorganic salt solution (1.0 g/L $FeSO_4{\cdot}7H_2O$, 1.0 g/L $MgCl_2{\cdot}6H_2O$, and 1.0 g/L $ZnSO_4{\cdot}7H_2O$, pH 7.2–7.4) for sporulation and on IWL4 plates (3.4% ISP4, 0.1% yeast extract, 0.4% tryptone, and 0.4% $MgCl_2{\cdot}6H_2O$, pH 7.2–7.4) for intergeneric conjugation at 30 °C. For the isolation of genomic DNA, *S. xinghaiensis* strains were cultivated in TSBY medium (3.0% tryptic soy broth, 10.3% sucrose, and 0.5% yeast extract) at 220 rpm and 30 °C.

Escherichia coli DH10B was used for plasmid construction. *E. coli* ET12567/pUZ8002 [32] was used as the donor strain for intergeneric conjugation. All *E. coli* strains were grown in Luria-Bertani (LB) liquid or on LB agar at 37 °C, and corresponding antibiotics (50 μg/mL apramycin or 50 μg/mL chloramphenicol) were added when necessary.

2.2. Construction of plasmids and S. xinghaiensis engineered strains

For the construction of *tlrC* overexpression plasmids pJPH08-1 and pJPH08-2, fragments of P_{tlrC}-*tlrC* or *kasO*p*-*tlrC* were amplified from the genomic DNA of *S. xinghaiensis* TL01 with primer pairs PC08-1 F/R or PC08-2 F/R. Then, the amplified fragments were inserted into pSET152 (digested with *BamHI* and *NotI*) separately using the ClonExpress One Step Cloning Kit (Vazyme, Nanjing, China). Similarly, fragments of $metK_{cs}$, $adoK_{cs}$-$metF_{cs}$, or *tylR* were amplified from the genomic DNA of TL01 using the primer pairs PC09 F/R, PC10 F/R, or PC12 F/R and assembled with pSET152-*kasO*p* (pJPH08-2 digested with *NdeI* and *BcuI*) separately to yield the $metK_{cs}$, $adoK_{cs}$-$metF_{cs}$, or *tylR* overexpression plasmids pJPH09, pJPH10, and pJPH12. The engineered DNA fragment of *kasO*p*-$metK_{cs}$ was amplified from pJPH09 with primer pair PC11 F/R and assembled with pJPH10 (digested with *Eco32I*) to obtain pJPH11.

pJPH01, pJPH17, pJPH23, and pJPH24 were constructed for combinational overexpression of *tlrC*, $metK_{cs}$, $adoK_{cs}$-$metF_{cs}$, and *tylR*. The 7977 bp genomic DNA containing *tlrC*, $metK_{cs}$, $adoK_{cs}$, $metF_{cs}$, and *tylR* with their native promoters was amplified with primer pair PC01 F/R and cloned into pSET152 (digested with *BamHI* and *NotI*) to generate pJPH01. The two engineered DNA fragments *kasO*p*-*tlrC* and *kasO*p*-*tylR* were amplified from pJPH08-2 and pJPH09 using primer pairs PC17 F1/R1 and PC17 F2/R2 and assembled with pJPH11 (digested with *Eco32I*) to generate pJPH17. Three fragments, $metK_{cs}$, $adoK_{cs}$-$metF_{cs}$, and *tylR*, were amplified from pJPH09, pJPH10, and pJPH11 using primer pairs PC23 F1/R1, PC23 F2/R2, or PC23 F3/R3 and cloned into pJPH08-2 (digested with *BamHI* and *BcuI*) to generate pJPH23. Additionally, three fragments, $metK_{cs}$, *kasO*p*-$adoK_{cs}$-$metF_{cs}$, and *tylR*, were amplified from pJPH09, pJPH10, and pJPH12 using primer pairs PC23 F1/R1, PC24 F1/R1, or PC24 F2/R2 and assembled with pJPH08-2 (digested with *BamHI* and *BcuI*) to generate pJPH24.

The recombinant plasmids and the vector pSET152 were transformed separately into the donor strain *E. coli* ET12567/pUZ8002 and introduced into TL01 via intergeneric conjugation according to the standard protocols [33], generating *S. xinghaiensis* engineered strains (Table S1). During the process of intergeneric conjugation, the plates were flooded with 25 μg/mL apramycin and 50 μg/mL trimethoprim after 14−16 h of incubation. After 4−5 days, the exconjugant single colonies were picked onto 2CM plates containing 25 μg/mL each of apramycin and nalidixic acid and confirmed using polymerase chain reaction (PCR).

2.3. Genomic sequencing of S. xinghaiensis TL01

For genomic sequencing, *S. xinghaiensis* TL01 was incubated in TSBY at 220 rpm and 30 °C for 48 h. Subsequently, the mycelium was collected via centrifugation at 5000 rpm for 10 min and washed thrice with phosphate buffered saline (PBS). Genomic DNA library preparation, Illumina sequencing, chromosome assembly, and annotation were performed at Shanghai Personal Biotechnology Co., Ltd. (Shanghai, China). The secondary metabolism-related gene clusters of *S. xinghaiensis* TL01 were analyzed using antiSMASH 5.0 (https://antismash.secondarymetabolites.org). The functions of the ORFs were predicted using the NCBI online BLAST program (http://blast.ncbi.nlm.nih.gov/) and 2ndFind (https://biosyn.nih.go.jp/2ndfind/). The whole genome of *S. xinghaiensis* TL01 has been deposited at GenBank under accession number CP121002.

2.4. Fermentation and quantitative analysis of tylosin

S. xinghaiensis TL01 and the engineered strains were grown on 2CM plates at 30 °C for 14 days, following which the agar cultures were inoculated into a 250 mL-shaking-flask containing 30 mL seed medium (0.4% yeast extract, 0.4% soybean powder, 1.2% corn steep liquor, 0.3% soybean oil (v/v), and 0.2% $CaCO_3$, pH 7.0) at 30 °C and 230 rpm for 48 h. Subsequently, 2 mL of the above seed culture was transferred to a 250

mL-shaking-flask with 30 mL fermentation medium (1.5% corn powder, 0.5% cottonseed powder, 1.0% fish powder, 0.05% betaine hydrochloride, 0.1% KCl, 0.1% NaCl, 0.04% $(NH_4)_2HPO_4$, 0.0004% $CoCl_2$, 0.0003% $NiSO_4$, 3.0% soybean oil (v/v), and 0.2% $CaCO_3$, pH 7.0), followed by cultivation at 230 rpm and 30 °C for 7 days.

Aliquots (1.0 mL) of the fermentation broth were collected and centrifuged at 12,000 rpm for 10 min, and subsequently, the supernatants were passed through 0.22-μm filters. The filtrate was diluted 10-fold for high performance liquid chromatography (HPLC) to analyze extracellular tylosin production. To analyze the intracellular production, 1.0 mL of methanol was added to the mycelia and incubated for 2 h with ultrasonic extraction; then, the supernatants were collected and passed through 0.22-μm filters for HPLC analysis. The production of tylosin was determined using an Agilent Series 1260 HPLC (Agilent Technologies, USA) with an Agilent ZROBAX SB-C18 (4.6 × 250 mm, 5 μm) column, with water containing 0.1% formic acid (solvent A) and acetonitrile (solvent B) as mobile phases. Samples (10 μL) were analyzed at a flow rate of 0.6 mL/min, with the following gradient: 0−5 min, 5−20% B; 5−25 min, 20−40% B; 25−30 min, 40−100% B; 30−35 min, 100% B; 35−40 min, 5% B. And they were detected at a wavelength of 286 nm.

2.5. Measurement of S. xinghaiensis strains biomass

The biomass of *S. xinghaiensis* strains was quantified by measuring DNA concentration using a simplified diphenylamine colorimetric method as described previously [34]. Cells were harvested from 1.0 mL culture aliquots at 24 h fermentation intervals, followed by centrifugation at 12,000 rpm for 10 min and washing thrice with deionized water. Then, the cells were resuspended in the diphenylamine reaction buffer (1.5 g diphenylamine, 100 mL glacial acetic acid, 1.5 mL concentrated sulfuric acid, and 1.0 mL 1.6% aqueous acetaldehyde) and vortexed for 1 min. The reactions were incubated for 1 h at 60 °C, followed by centrifugation for 2 min at 12,000 rpm. Subsequently, the supernatants were analyzed using the Infinite® M200Pro multimode microplate reader (Tecan, Switzerland) at OD_{595}. Three biological replicates were used.

2.6. Determination of intracellular SAM concentrations

Intracellular SAM concentrations of *S. xinghaiensis* strains were determined using liquid chromatography-tandem mass spectrometry (LC-MS/MS). Fermentation cultures (1.0 mL) were harvested 96 h after inoculation, followed by centrifugation at 12,000 rpm for 10 min at 4 °C. The supernatant was discarded, and intracellular SAM was extracted using 1.0 mL of 1.0 M formic acid at 4 °C for 1 h. Subsequently, the supernatant was collected after centrifugation at 12,000 rpm for 10 min at 4 °C and passed through 0.22-μm filters.

The supernatant was used for the determination of intracellular SAM concentrations with a Waters ACQUITY UPLC BEH C18 (100 × 2.1 mm, 1.7 μm) column using an UHPLC system (Shimadzu, Japan) and triple quadrupole 5500 mass spectrometer (AB Sciex, USA). The mobile phase consisted of water with 0.1% formic acid (solvent A) and acetonitrile with 0.1% formic acid (solvent B). Samples (1.0 μL) were analyzed at a flow rate of 0.5 mL/min with the following gradient: 0.5−3.0−4.0−5.0−7.0−7.1−9.0 min, 1.0%–1.0%−30%–100%−100%–1.0%−1.0% B. SAM was detected in a multiple reaction monitoring (MRM) mode with m/z parent > m/z daughter (399 > 298). Pure samples of SAM purchased from New England Biolabs were used as standards. Data were acquired and processed using Analyst 1.6.3 (AB Sciex, USA). Three biological replicates were used in the experiments.

2.7. Total RNA isolation and reverse transcription-quantitative PCR (RT-qPCR)

S. xinghaiensis cells were collected from 1.0 mL fermentation cultures at 96 h. The total RNA was extracted using the MolPure® Bacterial RNA Kit (Yeasen, Shanghai, China) according to the manufacturer's instructions. The quality of the RNA samples was determined using agarose gel electrophoresis and NanoDrop 2000 (Thermo Fisher Scientific, USA). Total RNA (about 1.0 μg) was used for reverse transcription using the HiScript III RT SuperMix for qPCR (plus gDNA wiper) (Vazyme, Nanjing, China). RT-qPCR was performed using ChamQ Universal SYBR qPCR Master Mix Q711-03 (Vazyme, Nanjing, China) on the Applied Biosystems 7500 system (Applied Biosystems, USA). The RNA polymerase sigma factor gene *hrdB* was used as the reference gene, and the relative levels of gene expression were quantified using the $2^{-\Delta\Delta CT}$ method [35]. Three biological replicates were used for each RT-qPCR analysis.

2.8. Transcriptome analysis

Samples (1.0 mL) of *S. xinghaiensis* strains (TLSET152, TLPH08-2, TLPH11, and TLPH17) were harvested at 96 h of fermentation, followed by centrifugation at 5000 rpm for 3 min and discarding of the supernatant. Subsequently, the cells were washed thrice with PBS and stored at −80 °C. The RNA isolation, transcriptome sequencing, and data analysis were conducted by Shanghai Biotechnology Corporation (Shanghai, China). The expression level of each gene was calculated as fragments per kilobase of transcript per million mapped reads (FPKM). Genes were determined as differentially expressed genes (DEGs) if the q-value <0.05 and $\log_2|\text{fold change}| > 1$. Three biological replicates were used for the transcriptome analysis of each strain. The raw transcriptomic data have been deposited in the NCBI Gene Expression Omnibus (GEO) database under accession number GSE228908.

3. Results

3.1. Genomic analysis of the industrial tylosin-producer S. xinghaiensis TL01

S. xinghaiensis strain TL01 is currently used for the industrial production of tylosin. The complete genome of TL01 consists of a single linear chromosome of 7,377,625 bp with a GC content of 73% (Fig. 1A). The TL01 genome contains five ribosomal RNA operons (5S–16S–23S) and 62 tRNA genes. The chromosomal replication initiator gene *dnaA* is situated at 3,827,155–3,829,017 bp, which is 138 kb on the right from the center of the chromosome.

According to antiSMASH prediction, the genome of *S. xinghaiensis* TL01 encodes 21 putative secondary metabolite biosynthetic gene clusters (BGCs), including three polyketide biosynthetic gene clusters, six nonribosomal peptide biosynthetic gene clusters, five terpene biosynthetic gene clusters, and gene clusters responsible for the synthesis of lanthipeptide, siderophore, or bacteriocin (Table S3). The tylosin biosynthetic gene cluster (*tyl* BGC) is located at the far left end of the TL01 chromosome, spanning a region of 87 kb (11,330–98,607 bp). The organization of all the *tyl* BGC genes of *S. xinghaiensis* TL01, *i.e.*, their order and transcriptional direction, is identical to the previously reported *tyl* BGC of *S. fradiae*, although its sequence has been reported as discontinuous segments rather than a contig [9]. The *S. xinghaiensis* TL01 tyl BGC contains 43 ORFs (Fig. 1B), including genes for the assembly and modification of the 16-membered lactone aglycone, synthesis and incorporation of three sugar moieties, transcriptional regulation, resistance, and tylosin efflux (Table S4).

3.2. Overexpression of the efflux gene tlrC increased tylosin production

In HPLC analysis of the fermentation broth of TL01, a large amount of tylosin (about 1.58 g per liter of broth, equal to 18% of the extracellular tylosin production) was observed to be associated with the mycelial pellet, which was inaccessible to the current industrial production process. To increase the extracellular production of tylosin, we

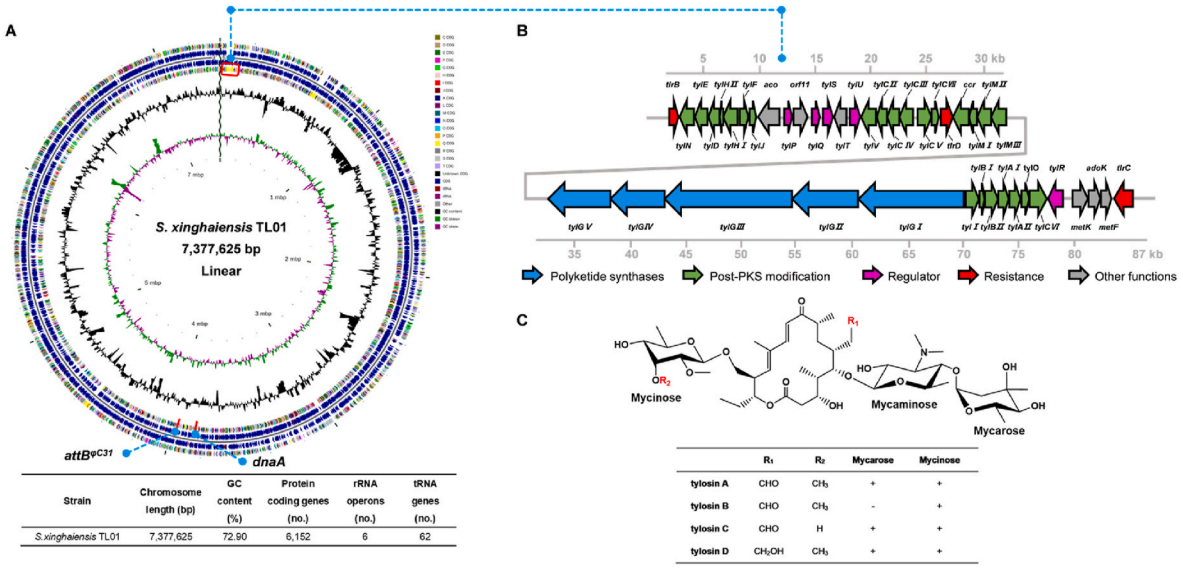

Strain	Chromosome length (bp)	GC content (%)	Protein coding genes (no.)	rRNA operons (no.)	tRNA genes (no.)
S.xinghaiensis TL01	7,377,625	72.90	6,152	6	62

	R_1	R_2	Mycarose	Mycinose
tylosin A	CHO	CH_3	+	+
tylosin B	CHO	CH_3	-	+
tylosin C	CHO	H	+	+
tylosin D	CH_2OH	CH_3	+	+

Fig. 1. The genomic features of *S. xinghaiensis* TL01, the biosynthetic gene cluster, and the structure of tylosin. **A** Diagram and general features of the TL01 genome. The circles represent (from inside to outside) the scale (kb), GC Skew, GC content, the COG of each CDS (the 4th and 7th circles), and the positions of CDS, tRNA, and rRNA in the genome (the 5th and 6th circles). **B** Schematic diagram of the tylosin gene cluster. Arrows indicate genes and their directions. Genes for polyketide synthases are colored in blue, for post-PKS modification are colored in green, for regulators are colored in pink, for antibiotic resistance are colored in red, and for other functions are colored in gray. **C** Structures of tylosin A, B, C, and D.

constructed two mutants, TLPH08-1 and TLPH08-2, by integrating an additional copy of the tylosin efflux gene *tlrC* under the control of the native promoter P_{tlrC} or the strong constitutive promoter *kasO*p* in the *S. xinghaiensis* TL01 chromosome.

As shown in Fig. 2B, the extracellular tylosin production of TLPH08-1 (9.53 g/L) and TLPH08-2 (10.51 g/L) was increased by 7% and 18%, respectively, compared to that of the original strain TL01. In particular, the ratio of intracellular to extracellular tylosin decreased significantly in TLPH08-1 (15%) and TLPH08-2 (10%) compared to that in TL01 (18%) (Fig. S1). Integration of the empty vector did not affect the production of tylosin in the resultant strain, TLSET152. To investigate the influence of *tlrC* overexpression on tylosin fermentation, we determined the extracellular tylosin production and biomass of TLPH08-2, TL01, and TLSET152 at an interval of 24 h until 168 h. We observed that TLPH08-2 produced more extracellular tylosin throughout the fermentation process (Fig. 2C). The biomass of TLPH08-2 was slightly better than that of TL01 and TLSET152, although the difference was not statistically significant. These results suggested that overexpression of *tlrC* enhanced the production of extracellular tylosin by increasing tylosin export and thereby reducing the putative feedback inhibition.

3.3. Enhancing tylosin production by improving SAM biosynthesis or overexpressing the pathway specific activator gene tylR

The tylosin biosynthetic pathway involves multiple methyl transfer steps catalyzed by SAM-dependent methyltransferases, in which SAM acts as the co-substrate and methyl donor [10]. Coincidentally, the TL01 tylosin BGC contains a putative operon encoding paralogs of SAM synthetase ($metK_{cs}$), adenosine kinase ($adoK_{cs}$), and 5,10-methylenetetrahydrofolate reductase ($metF_{cs}$) belonging to the methionine cycle and folate cycle that are primarily involved in the biosynthesis of SAM (Fig. 2A). The subscript ***cs*** indicates they are **c**luster-**s**ituated paralogs. To improve the SAM supply in *S. xinghaiensis* TL01, additional copies of these genes in the form of *kasO*p*-$metK_{cs}$ or *kasO*p*-$adoK_{cs}$-$metF_{cs}$ were integrated into the chromosome of TL01 using pSET152 as the vector, yielding the mutants TLPH09 and TLPH10, respectively. Further, *kasO*p*-$metK_{cs}$ and *kasO*p*-$adoK_{cs}$-$metF_{cs}$ were integrated together in TL01 to yield a combined overexpression mutant TLPH11.

HPLC analysis revealed that the extracellular tylosin production of TLPH09, TLPH10, and TLPH11 increased by 12%, 11%, and 22%, respectively (Fig. 2B). Among these mutants, the combined engineered strain TLPH11 overexpressing both $metK_{sc}$ and the $adoK_{sc}$-$metF_{sc}$ operon yielded the highest level of tylosin (10.87 g/L). To determine the SAM supply in TLPH11, we quantified the intracellular SAM content using LC-MS/MS. As expected, the intracellular SAM concentration of TLPH11 was 78.43 μmol/kg cell dry weight, which was significantly enhanced by 1.86-fold compared to that of TL01 (27.42 μmol/kg cell dry weight) (Fig. S2). The production curves confirmed the increase in tylosin titer in TLPH11. In particular, the tylosin production titer of TLPH11 was consistently higher than that of the starting strain TL01 and the vector control TLSET152 at all time points (24−168 h) (Fig. 2C). The biomass of TLPH11 did not differ from that of TL01 or the vector control, suggesting that the growth of TLPH11 was not significantly affected (Fig. 2D).

In addition, TylR is a pathway-specific activator that directly activates transcription of tylosin biosynthetic genes and is positively related to tylosin production [25]. Accordingly, we integrated a copy of *kasO*p*-*tylR* into the TL01 chromosome. The resultant mutant TLPH12 produced 11% more tylosin than TL01. The biomass of TLPH12 was not affected compared to that of TL01 or the vector control (Fig. 2D).

3.4. Combinational overexpression of multiple genes elevated the production of tylosin

To further improve tylosin production, the engineered gene cassettes *kasO*p*-*tlrC*, *kasO*p*-$metK_{cs}$, *kasO*p*-$adoK_{cs}$-$metF_{cs}$, and *kasO*p*-*tylR* were combined and integrated into TL01, generating the mutant strain TLPH17. We also integrated an additional copy of *tlrC*, $metK_{cs}$, $adoK_{cs}$-$metF_{cs}$, and *tylR* under their native promoters in TL01 to generate TLPH01. Compared to that of TL01, extracellular tylosin production was increased by 14% in TLPH01 (10.11 g/L) and by 23% in TLPH17 (10.93 g/L) (Fig. 3A), suggesting an advantage of the strong promoter *kasO*p* over the native promoters for overexpression. However, TLPH17 only achieved a small increment (4.5%, $P < 0.05$) in tylosin production over the efflux-overexpressing strain TLPH08-2 and differed negligibly (0.41%, $P > 0.05$) from the SAM biosynthetic gene-overexpressing strain

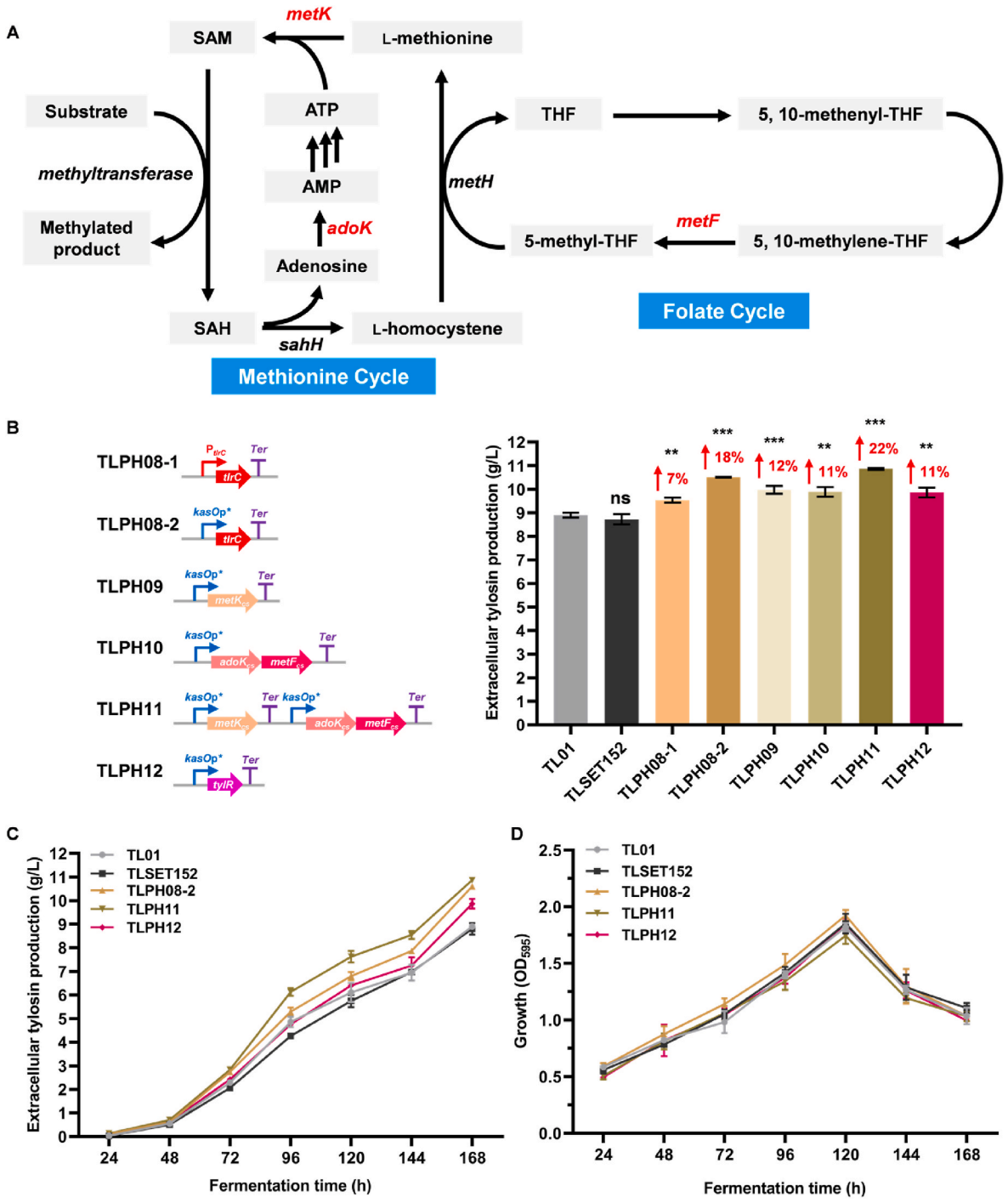

Fig. 2. Effects of single overexpression of the tylosin efflux gene *tlrC*, SAM biosynthetic genes, and pathway-specific activator gene *tylR* on tylosin production and cell growth. **A** The regeneration of SAM through the methionine cycle and the folate cycle. SAM, *S*-adenosyl methionine. SAH, *S*-adenosylhomocysteine. THF, Tetrahydrogen folic acid. 5-methyl-THF, 5-methyltetrahydrofolate. 5,10-methylene-THF, 5,10-methylenetetrahydrofolate. **B** The extracellular tylosin production of TLPH08-2, TLPH11, and TLPH12 at 168h after inoculation. The red arrows and numbers show the percentage increase in extracellular tylosin production of the mutants compared to the original strain TL01. Differences between each engineering strain and the original strain TL01 were analyzed by the unpaired Student's *t*-test. $^{*}P < 0.05$, $^{**}P < 0.01$, $^{***}P < 0.001$, and "ns" means not significant for comparison with the original strain TL01. **C, D** Time course of extracellular tylosin production and biomass of TLPH08-2, TLPH11, and TLPH12. The error bars depict the standard deviations of three biological replicates.

TLPH11. This indicated that the combinational overexpression of the five genes in TLPH17 resulted in a poor additive effect on the elevation of extracellular tylosin production compared to the single overexpression of the efflux or the SAM biosynthetic pathway. Consistently, the ratio of intracellular to extracellular tylosin in TLPH17 (13%) was determined to be significantly higher than that in the efflux-overexpressing strain TLPH08-2 (10%) (Fig. S1). The intracellular SAM content in TLPH17 (56.31 μmol/kg cell dry weight) was lesser than that of the SAM-overproducing strain TLPH11 (78.43 μmol/kg cell dry weight), although it was higher than those of TL01 and TLPH01 (Fig. S2). These results largely attributed the poor additive effect of TLPH17 to its lower tylosin efflux compared to that of TLPH08-2 and lesser SAM supply compared to that of TLPH11.

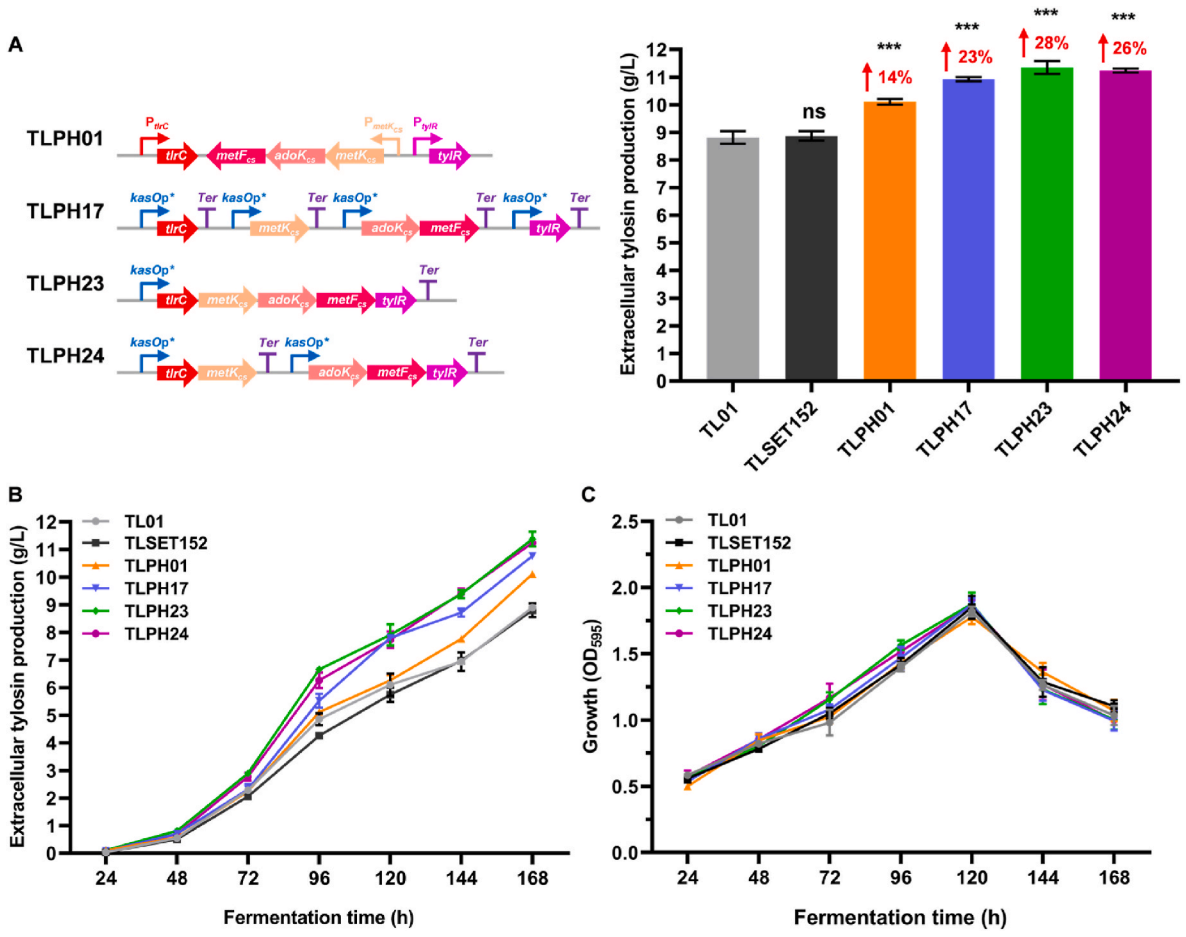

Fig. 3. Effects of combinational overexpression of the tylosin efflux gene *tlrC*, cluster-situated SAM biosynthetic genes, and pathway-specific activator gene *tylR* on tylosin production and cell growth. **A** The extracellular tylosin production of TLPH01, TLPH17, TLPH23, and TLPH24 at 168 h after inoculation. The red arrows and numbers show the percentage increase in extracellular tylosin production of the mutants compared to the original strain TL01. Differences between each engineering strain and the original strain TL01 were analyzed by the unpaired Student's *t*-test. $^{*}P < 0.05$, $^{**}P < 0.01$, $^{***}P < 0.001$, and "ns" means not significant for comparison with the original strain TL01. **B, C** Time course of extracellular tylosin production and biomass of TLPH01, TLPH17, TLPH23, and TLPH24. The error bars depict the standard deviations of three biological replicates.

3.5. Transcriptional analysis of three high tylosin-producing strains

To understand the differences in gene expression associated with the improvement in tylosin production and the reason underlying the poor additive effect from combinational overexpression in TLPH17, the transcriptomes of three high tylosin-producing engineered strains (TLPH08-2, TLPH11, and TLPH17) and the vector control strain TLSET152 at 96 h of fermentation were analyzed using RNA-Seq.

First, the tylosin BGC in all strains was highly expressed, corroborating hyperproduction of tylosin. For example, in the vector control strain TLSET152, 27 of 154 highly expressed chromosomal genes (FPKM>1000) in the transcriptome were located in tylosin BGC, while only three tylosin BGC genes (*tlrB*, *tylQ*, and *tylC VII*) were poorly expressed (FPKM<100). Interestingly, we observed that the expression level of 27 of 43 genes in the tylosin BGC was significantly higher in TLPH08-2, TLPH11, and TLPH17 ($P<0.05$, fold change = 1.4–12.9), including the engineered target genes *tlrC* in TLPH08-2, $metK_{cs}$ and $adoK_{cs}$-$metF_{cs}$ in TLPH11 and TLPH17 ($P<0.05$, fold change>2.0), and all tylosin biosynthetic genes except for the *tylGI-ccr* operon genes (Fig. 4). Surprisingly, the RNA-Seq data indicated lack of any obvious difference between the *tlrC* expression (FPKM values) of TLPH17 and the vector control TLSET152. However, the RT-qPCR analysis showed that the expression level of *tlrC* in TLPH17 was significantly higher than that in TLSET152 (Fig. 5), which was consistent with the data on the intracellular to extracellular tylosin ratio presented in Fig. S1. In addition, we also found that the expression levels of the five engineered genes in TLPH17 were lower than those of *tlrC* in TLPH08-2, $metK_{cs}$, $adoK_{cs}$, and $metF_{cs}$ in TLPH11, and *tylR* in TLPH12, respectively (Figs. 4 and 5).

Second, the differentially expressed genes (DEGs) between the engineered strains and the vector control TLSET152 were analyzed. In total, 668 genes (406 upregulated and 262 downregulated genes), 545 genes (339 upregulated and 206 downregulated genes), and 940 genes (585 upregulated and 355 downregulated genes) were identified as DEGs in TLPH08-2, TLPH11, and TLPH17, respectively. The DEGs shared by the three mutant strains consisted of 158 co-upregulated genes and 105 co-downregulated genes (Fig. 6A and B). Among these, 16 transporter-associated genes located outside the tylosin BGC were co-upregulated, two of which (*sxh3073* and *sxh3442*) encoded multidrug ATP-binding cassette ABC transporters. Multidrug efflux pumps from various families can improve multiple antibiotic resistance or drug transport abilities in bacteria [36]. In TLPH08-2, TLPH11, and TLPH17, the relative expression levels of *sxh3073* and *sxh3442* were all significantly increased compared to those in the control ($P<0.05$) (Fig. 6C), suggesting that these genes may promote the efflux of tylosin, thereby reducing the possible negative effect of tylosin on cell metabolism. In addition, 28 genes located in four antiSMASH-predicted secondary metabolic BGCs were co-downregulated in these mutants (Table S5), which might save intracellular resources for tylosin synthesis.

Third, Gene ontology (GO) and Kyoto Encyclopedia of Genes and Genomes (KEGG) enrichment were used to analyze the DEGs and their

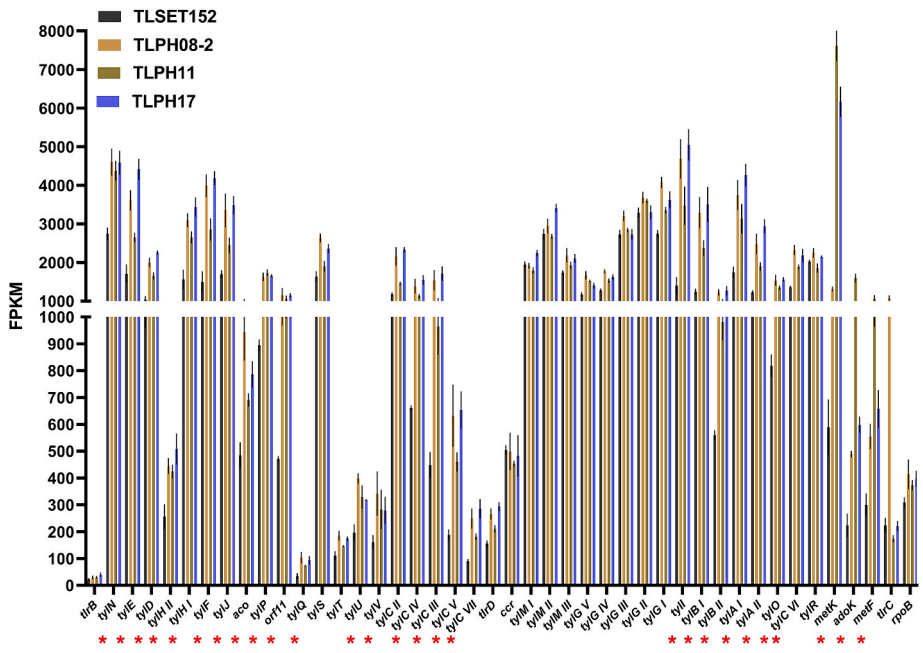

Fig. 4. Gene expression values (FPKM) of genes of the tylosin BGC in TLPH08-2, TLPH11, TLPH17, and TLSET152 (vector control). RNA samples were extracted from the fermentation broth of different strains 96 h after inoculation. *rpoB*, RNA polymerase β subunit gene. Stars indicate that the gene's FPKM values in three mutants were all higher than the vector control ($P < 0.05$). The error bars depict the standard deviations of three biological replicates.

main biological functions. The GO terms of DEGs were mainly enriched in the catalytic activity in the molecular function category, the cell and cell part in the cellular component category, and the metabolic process and the cellular process in the biological process category in three engineered strains (Fig. 7A, **C**, and **E**). The DEGs were mainly involved in various types of secondary metabolites biosynthesis, lipid metabolism, starch and sucrose metabolism, C5-branched dibasic acid metabolism, ABC transporters, one carbon pool by folate, and other pathways in three engineered strains (Fig. 7B, **D**, and **F**). These suggested that cell growth, energy metabolism, and other primary metabolic processes were accelerated, thereby increasing energy and precursor supplies for tylosin synthesis.

3.6. Fine-tuning the co-overexpression of multiple genes further enhanced tylosin production

In TLPH17, the co-overexpressed target genes were divided into four transcription units, each of which was under the control of the strong constitutive promoter *kasO*p*, followed by a terminator. As revealed by the RNA-seq and RT-qPCR data, TLPH17 showed limited *tlrC* expression compared to TLPH08-2 and lower expression of $adoK_{cs}$ and $metF_{cs}$ than TLPH11, which might account for the poor additive effect of combinational co-overexpression on tylosin production. We proposed that optimization of the transcriptional organization of these target genes would further improve the efflux of tylosin and SAM supply, thereby boosting extracellular tylosin production. Therefore, we constructed two mutant strains, TLPH23 and TLPH24, in which the target genes were combined into one or two transcription units for their overexpression.

As presented in Fig. 3, the extracellular tylosin production of TLPH23 and TLPH24 reached up to 11.35 and 11.24 g/L, which were further improved by 5.1% and 3.9% compared to that of TLPH17. In particular, the TLPH23 produced the highest amount of tylosin among all the 10 mutant strains constructed in this study. RT-qPCR analysis revealed that the transcription levels of *tlrC*, $adoK_{cs}$, and $metF_{cs}$ were improved in TLPH23, and that the transcription levels of *tlrC* and $adoK_{cs}$ were improved in TLPH24 compared to those in TLPH17 (Fig. 5). In particular, the relative expression level of *tlrC* in TLPH23 and TLPH24 was increased by 1.5-fold and 1.4-fold, respectively. Consistently, their ratio of intracellular to extracellular tylosin decreased to 12%, compared to 14% for TLPH17 (Fig. S1). Nonetheless, the intracellular SAM concentration in TLPH23 and TLPH24 did not change significantly compared to that of TLPH17 (Fig. S2). Overall, these results indicated that the transcription levels of multiple co-overexpressed genes can be fine-tuned by optimizing the transcription units, which in turn boosts the extracellular production of tylosin.

5Discussion

Improving the fermentation titer of structurally complex secondary metabolites such as tylosin is urgently required, especially in high-producing industrial strains. In this study, after analyzing the intact biosynthetic gene cluster from the tylosin hyperproducer *S. xinghaiensis* TL01, we successfully increased the fermentation titer of this industrial strain by 28% via combinatorial overexpression of the cluster-situated genes for SAM supply, final product efflux, and positive regulation.

Enhancement of SAM supply by exogenous addition of SAM, SAM biosynthesis precursor L-methionine, or overexpression of SAM synthetase (MetK) has been shown to increase the production of various secondary metabolites, such as streptomycin [37], ansamitocin P-3 [38], erythromycin [39], nosiheptide [40], avermectin [41], lincomycin [42], and cephalosporin C [43]. Remarkably, combinatorial engineering of SAM synthetase genes, SAM degradation genes, L-methionine synthetase, and transporter genes elevated bacitracin production in an industrial strain that already produced high levels of bacitracin [44]. However, in another study, co-overexpression of five putative SAM biosynthetic genes (*metK*, *adoK*, *metH*, *metF*, and *sahH*) did not significantly boost the production of novobiocin; instead, these resulted in the accumulation of high concentrations of SAM and negatively affected the viability of the engineered strain in the stationary phase [45]. The tylosin biosynthetic pathway involves four SAM-dependent methyltransferases, namely TylCIII, TylMI, TylE, and TylF [10]. The industrial strain *S. xinghaiensis* TL01 harbors three SAM cycle paralog-coding genes, $metK_{cs}$, $adoK_{cs}$, and $metF_{cs}$, organized as a putative operon in the tylosin BGC, in addition to a full set of five SAM biosynthetic orthologs scattered around the chromosome, namely, *metK* (*sxh5659*), *metH* (*sxh5462*), *metF* (*sxh5033*), *adoK* (*sxh4973*), and *sahH* (*sxh4023*).

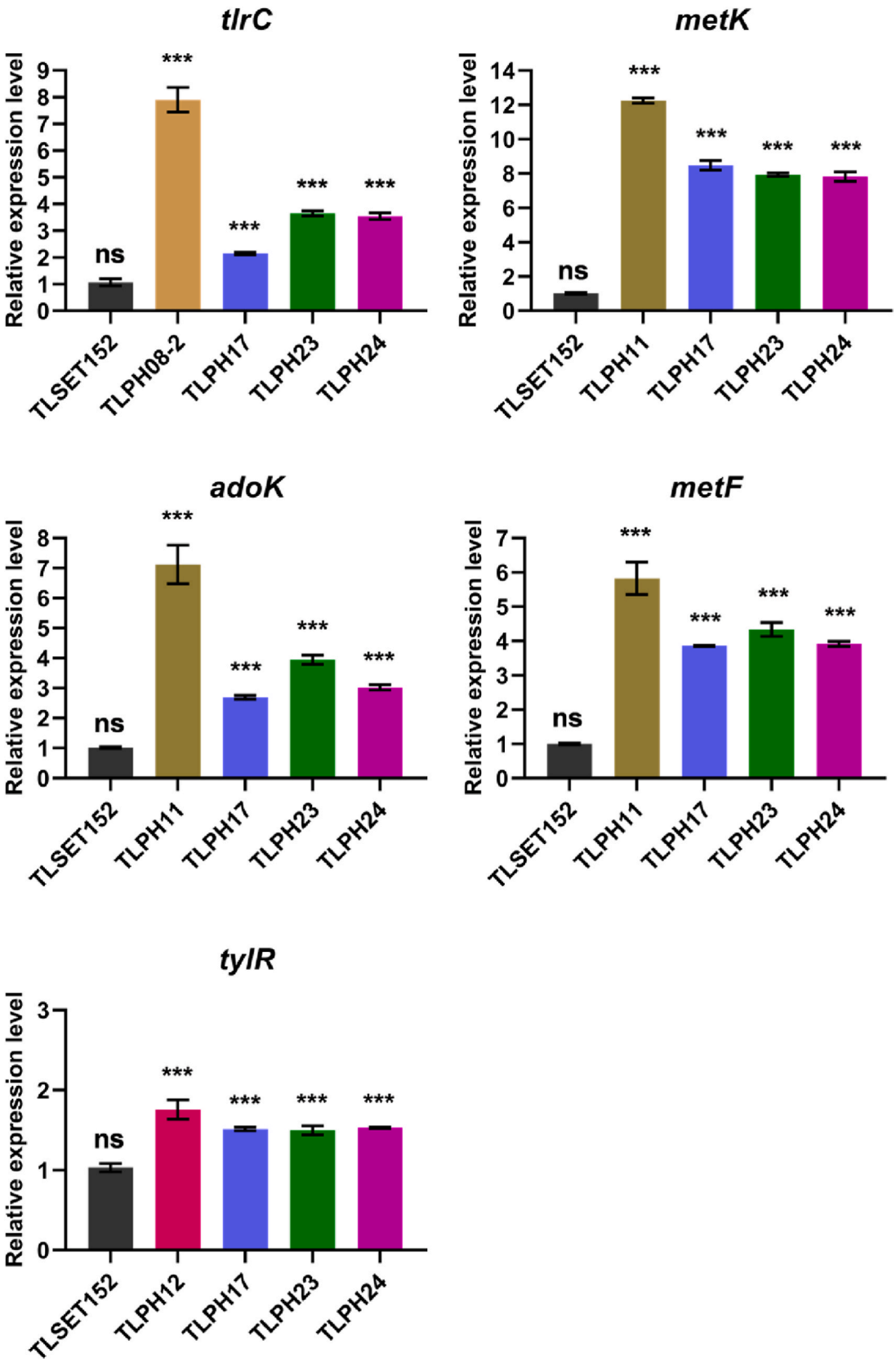

Fig. 5. RT-qPCR analysis of the transcriptional levels of *tlrC*, $metK_{cs}$, $adoK_{cs}$, $metF_{cs}$, and *tylR* in *S. xinghaiensis* strains. RNA samples were extracted from the fermentation broth of different strains 96 h after inoculation. The relative level of target genes was normalized to the RNA polymerase sigma factor gene *hrdB*. Differences between each engineering strain and the original strain TL01 were analyzed by the unpaired Student's *t*-test. $^{*}P < 0.05$, $^{**}P < 0.01$, $^{***}P < 0.001$, and "ns" means not significant for comparison with the original strain TL01. The error bars depict the standard deviations of three biological replicates.

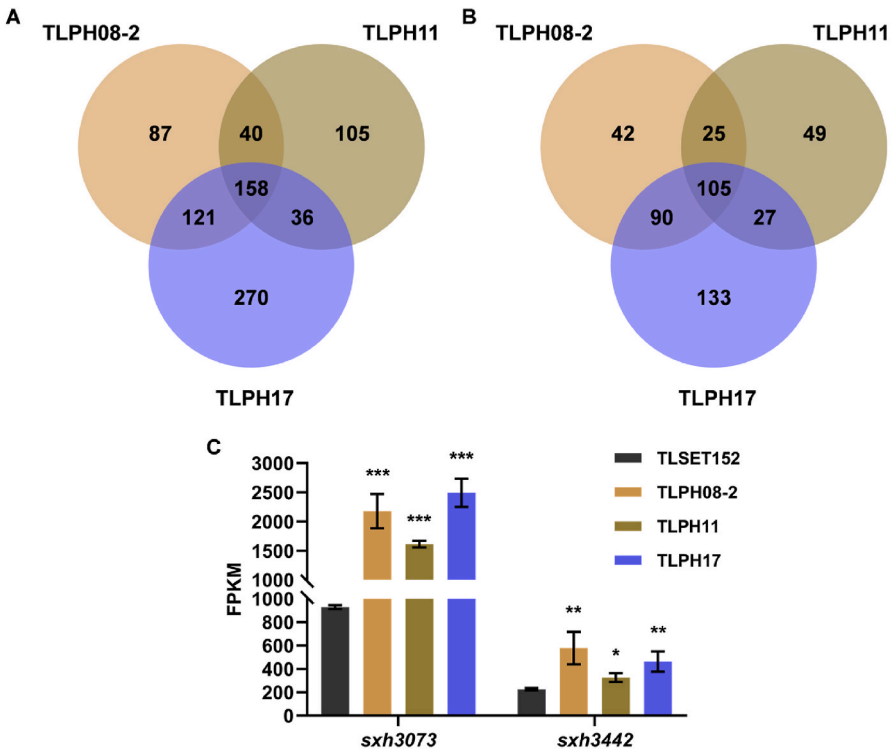

Fig. 6. Analysis of differentially expressed genes in TLPH08-2, TLPH11, and TLPH17 compared to the vector control TLSET152. **A** Venn diagram of the number of upregulated genes. **B** Venn diagram of the number of downregulated genes. **C** Expression values (FPKM) of two multidrug ABC transporter genes. Differences between each engineering strain and the vector control TLPSET152 were analyzed by the unpaired Student's *t*-test. $^{*}P < 0.05$, $^{**}P < 0.01$, $^{***}P < 0.001$. The error bars depict the standard deviations of three biological replicates.

In this study, we demonstrated that overexpression of $metK_{cs}$ alone or $adoK_{cs}$-$metF_{cs}$ alone elevated intracellular SAM concentrations and extracellular tylosin production. Co-overexpression of $metK_{cs}$ and $adoK_{cs}$-$metF_{cs}$ led to a promising elevation of 22% (in TLPH11) compared to the yield of the starting industrial strain (8.90 g/L). Furthermore, the overexpression of the cluster-situated SAM biosynthetic genes did not exert any obvious detrimental effect on the growth of the resultant strains TLPH11, TLPH17, TLPH23, and TLPH24 (Figs. 2 and 3). We assumed that the remarkable increase in SAM production in these engineered strains is rapidly utilized by the tylosin biosynthetic pathway, resulting in higher production of tylosin, because of which SAM cannot accumulate to a harmful level and does not cause any obvious detrimental effect on cell growth. In fact, the SAM concentration in our engineered strains was considerably lower than the reported detrimental level in *Streptomyces* [45]. Therefore, we speculated that further increasing the expression of these SAM biosynthetic genes would probably further promote the production of tylosin. Nevertheless, data from this study and a previous study [44] encourage combinational overexpression of SAM biosynthetic genes to support substantial SAM production and utilization in high-producing industrial strains.

SAM plays an important role in many intracellular biochemical processes in addition to acting as a methyl donor for methylation. Several previous studies suggested the involvement of SAM in the transcriptional regulation of secondary metabolite biosynthesis to increase the expression level of the biosynthetic genes [37,44,46]. In our study, the transcriptome analysis revealed that the expression level of 27 of 43 tylosin biosynthetic genes was also elevated by the overexpression of SAM biosynthetic genes in TLPH11 and TLPH17 (Fig. 4), although the specific mechanism is yet to be investigated.

Efflux plays a key role in the secretion of the end product and the avoidance of self-toxicity. Overexpression of gene cluster-situated transporter genes was demonstrated to be an effective strategy to enhance the production of avermectin in a high-yield strain [20,47]. In this study, we also demonstrated that overexpression of the BGC-situated transporter gene *tlrC* improved extracellular production and reduced the ratio of intracellular tylosin significantly. In a recent study, Wang et al. identified six ansamitocin P-3 (AP-3) efflux genes outside the biosynthetic BGC using comparative transcriptomic analysis. Overexpression of four of these genes led to the enhancement of AP-3 production [48]. Our transcriptome analysis revealed that the expression level of two multidrug ABC transporter genes (*sxh3073* and *sxh3442*) outside the tylosin BGC was significantly increased in three tylosin-overproducing engineered strains (TLPH08-2, TLPH11, and TLPH17). Further experiments are required to determine whether *sxh3073* and *sxh3442* are involved in tylosin exportation. Finally, we observed that the *S. xinghaiensis* TL01 strain was tolerant to high concentrations of tylosin (25 g/L, data not shown). Therefore, the improvement of fermentation titer due to *tlrC* overexpression may be because of the alleviation of the possible negative feedback regulation of tylosin on the biosynthetic pathway rather than because of the avoidance of self-toxicity.

Manipulation of regulatory genes, such as overexpression of positive regulator genes or removal of repressor genes, is another effective strategy for enhancing the production of secondary metabolites [49]. Tylosin biosynthesis is under the complex control of five cluster-situated regulators, among which TylR regulates the transcription of tylosin BGC directly [25]. In this study, we demonstrated that overexpression of *tylR* led to a moderate enhancement of tylosin production to 9.86 g/L (about 11% higher than that by TL01), although *tylR* was already expressed at a high level in the starting strain TL01.

Based on the above positive results, combination overexpression was the next rational step for further improving the titer. However, the simple combination of the SAM biosynthetic genes ($metK_{cs}$, $adoK_{cs}$, and $metF_{cs}$), the tylosin efflux gene (*tlrC*), and the pathway-specific activator gene (*tylR*) failed to achieve a satisfying additive effect on the elevation of tylosin production. At first glance, this phenomenon was similar to a recent study performed in *S. venezuelae*, in which the engineering of multiple genes did not result in a synergic effect [26]. Our subsequent transcriptional analysis showed that the expression levels of *tlrC* and SAM biosynthetic genes in the combinatorial strain TLPH17 were lower than those in the singly overexpressed strains TLPH08-2 and TLPH11, respectively, which in turn resulted in poorer tylosin efflux in TLPH17

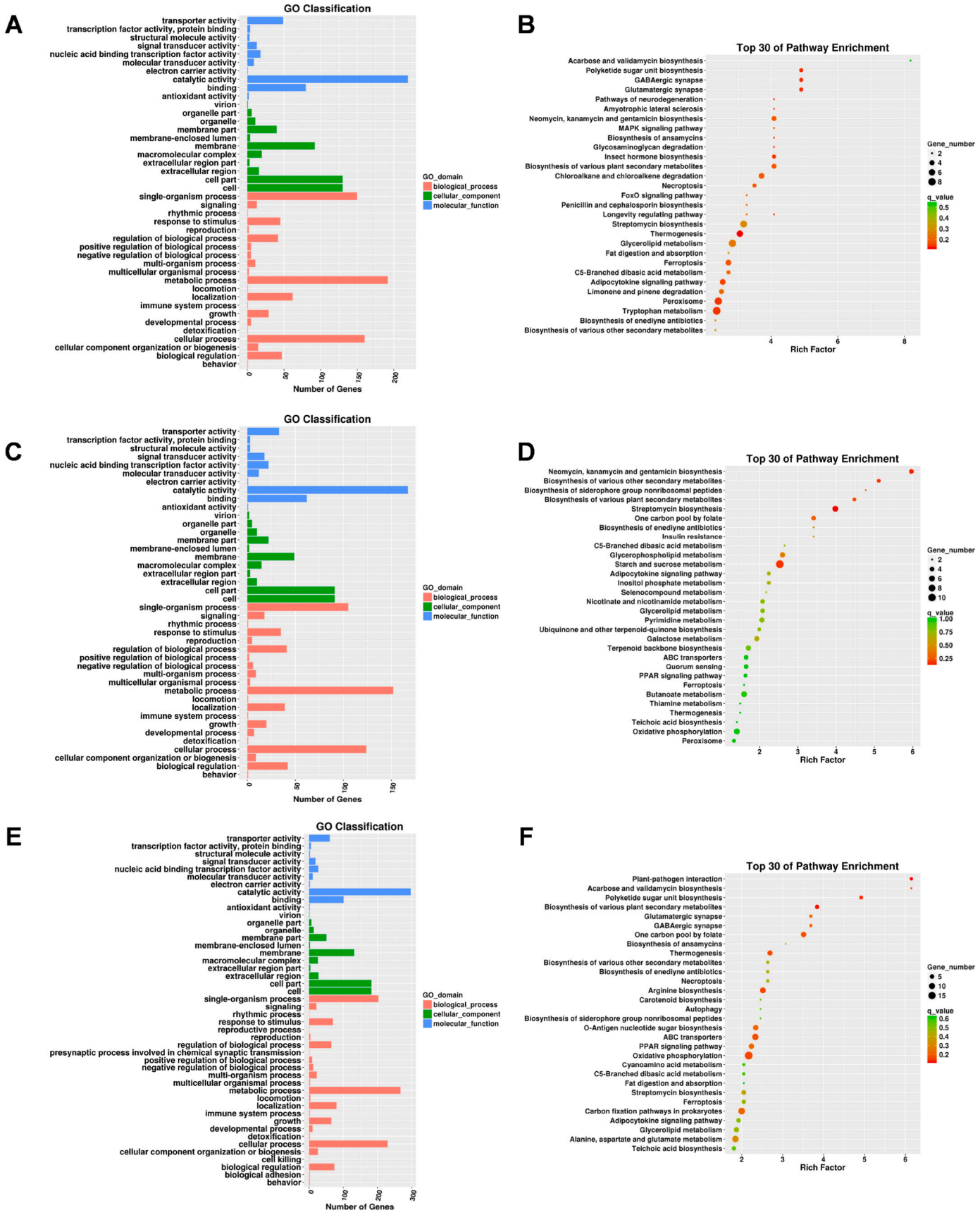

Fig. 7. GO enrichment and KEGG enrichment of differentially expressed genes in TLPH08-2, TLPH11, and TLPH17 compared to the vector control TLSET152. **A, C, E** GO enrichment of DEGs in TLPH08-2, TLPH11, and TLPH17. **B, D, F** KEGG enrichment of DEGs in TLPH08-2, TLPH11, and TLPH17.

than in TLPH08-2 and poorer SAM supply than in TLPH11. We hypothesized that the presence of multiple strong constitutive promoters within a relatively narrow DNA region, such as in TLPH17, would possibly lead to detrimental competition for RNA polymerase among the corresponding transcriptional units. Subsequently, the expression levels of five target genes were fine-tuned by rearranging them into one or two transcripts in TLPH23 and TLPH24, resulting in a slight increase in the relative expression levels of *tlrC* and $adoK_{cs}$ compared to those in TLPH17 (Fig. 5). However, the transcriptional levels of five target genes were still lower than those of *tlrC* in TLPH08-2, SAM biosynthetic genes in TLPH11, and *tylR* in TLPH12. We speculated that the length of each transcription unit and the order of target genes might also be critical factors affecting the transcription levels, and more in-depth research is required to further coordinate the expression levels of the target genes.

Our research presents an effective combinatorial metabolic engineering strategy to increase the production of tylosin in a hyper-producing industrial strain. This approach and the SAM-overexpression plasmids could be applied to enhance the production of other valuable natural products.

CRediT authorship contribution statement

Penghui Dai: Designed the project, Performed the experiments, Processed the data and plotted the figures, Writing - original draft, Writing - review & editing. **Yuyao Qin**, **Luyuan Li**, **Haidi Li, Danying Xu, Yuqing Song**: Performed the experiments. **Lihuo Lv**: Data analysis. **Tingting Huang**: Data analysis. **Shuangjun Lin**: Data analysis, Writing - review & editing. **Zixin Deng**: Designed the project. **Meifeng Tao**: Designed the project, Data analysis, Writing - review & editing.

Declaration of competing interest

The authors indicate that they have no conflict of interest.

Acknowledgments

This work was supported by the National Key Research and Development Program of China (grant no. 2022YFC210540303) and the “Major Project” of Haihe Laboratory of Synthetic Biology (22HHSWSS00001).

Appendix A. Supplementary data

Supplementary data to this article can be found online at https://doi.org/10.1016/j.synbio.2023.07.002.

References

[1] Arsic B, Barber J, Čikoš A, Mladenovic M, Stankovic N, Novak P. 16-membered macrolide antibiotics: a review. Int J Antimicrob Agents 2018;51(3):283–98. https://doi.org/10.1016/j.ijantimicag.2017.05.020.

[2] Wu JX, Zhang CL, Xu JL, Zhang GD, Hao J, Zhang M, Song M, Qi P, Zhang G, Liang JL. Bioconversion, purification and characterization of tylvalosin. Chem Pap 2017;71:2283–91. https://doi.org/10.1007/s11696-017-0222-8.

[3] Poehlsgaard J, Andersen NM, Warrass R, Douthwaite S. Visualizing the 16-membered ring macrolides tildipirosin and tilmicosin bound to their ribosomal site. ACS Chem Biol 2012;7(8):1351–5. https://doi.org/10.1021/cb300105p.

[4] Hamill RL, Haney ME, Stamper M, Wiley PF. Tylosin, a new antibiotic. II. Isolation, properties, and preparation of desmycosin, a microbiologically active degradation product. Antibiot Chemother 1961;11:328–34.

[5] Jensen AL, Darken MA, Schultz JS, Shay AJ. Relomycin: flask and tank fermentation studies. Antimicrob Agents Chemother 1963;161:49–53.

[6] Pape H, Brillinger GU. Stoffwechselprodukte von Mikroorganismen. Arch Mikrobiol 1973;88(1):25–35. https://doi.org/10.1007/BF00408838.

[7] Bekker OB, Vatlin AA, Zakharevich NV, Lysenkova LN, Shchekotikhin AE, Danilenko VN. Draft genome sequence of *Streptomyces xinghaiensis* (*fradiae*) OlgR, a strain resistant to oligomycin A. Microbiol Res Ann 2019;8(2):e01531-18. https://doi.org/10.1128/MRA.01531-18.

[8] Vatlin AA, Bekker OB, Lysenkova LN, Shchekotikhin AE, Danilenko VN. Bioinformatics analysis of genes of *Streptomyces xinghaiensis* (*fradiae*) ATCC 19609 with a focus on mutations conferring resistance to oligomycin A and its derivatives. J Glob Antimicrob Resist 2020;22:47–53. https://doi.org/10.1016/j.jgar.2020.01.026.

[9] Cundliffe E, Bate N, Butler A, Fish S, Gandecha A, Merson-Davies L. The tylosin-biosynthetic genes of *Streptomyces fradiae*. Antonie Leeuwenhoek 2001;79(3):229–34. https://doi.org/10.1023/A:1012065300116.

[10] Kim E, Song MC, Kim MS, Beom JY, Lee EY, Kim DM, et al. Characterization of the two methylation steps involved in the biosynthesis of mycinose in tylosin. J Nat Prod 2016;79(8):2014–21. https://doi.org/10.1021/acs.jnatprod.6b00267.

[11] Cundliffe Eric. Control of tylosin biosynthesis in *Streptomyces fradiae*. J Microbiol Biotechnol 2008;18(9):1485–91. https://koreascience.kr/article/JAKO200835054212208.page.

[12] Bate N, Bignell DRD, Cundliffe E. Regulation of tylosin biosynthesis involving ‘SARP-helper’ activity. Mol Microbiol 2006;62(1):148–56. https://doi.org/10.1111/j.1365-2958.2006.05338.x.

[13] Bate N, Butler AR, Gandecha AR, Cundliffe E. Multiple regulatory genes in the tylosin biosynthetic cluster of *Streptomyces fradiae*. Chem Biol 1999;6(9):617–24. https://doi.org/10.1016/S1074-5521(99)80113-6.

[14] Khaliq S, Akhtar K, Afzal Ghauri M, Iqbal R, Mukhtar Khalid A, Muddassar M. Change in colony morphology and kinetics of tylosin production after UV and gamma irradiation mutagenesis of *Streptomyces fradiae* NRRL-2702. Microbiol Res 2009;164(4):469–77. https://doi.org/10.1016/j.micres.2007.02.005.

[15] Khaliq S, Ghauri MA, Akhtar K. Characterization of mutations in regulatory genes of *Tyl* cluster leading to overexpression of tylosin in mutant γ-1 of *Streptomyces fradiae* NRRL-2702. Appl Microbiol Biotechnol 2014;98(2):785–93. https://doi.org/10.1007/s00253-013-5317-8.

[16] Choi Dubok, On You C, Mitsuyasu O. Tylosin production by *Streptomyces fradiae* using raw cornmeal in airlift bioreactor. J Microbiol Biotechnol 2007;17(7):1071–8. https://koreascience.kr/article/JAKO200734514830103.page.

[17] Choi DB, Tamura S, Park YS, Okabe M, Seriu Y, Takeda S. Efficient tylosin production from *Streptomyces fradiae* using rapeseed oil. J Ferment Bioeng 1996;82(2):183–6. https://doi.org/10.1016/0922-338X(96)85047-1.

[18] Zhang YX, Perry K, Vinci VA, Powell K, Stemmer WPC, del Cardayré SB. Genome shuffling leads to rapid phenotypic improvement in bacteria. Nature 2002;415(6872):644–6. https://doi.org/10.1038/415644a.

[19] Lu C, Zhang X, Jiang M, Bai L. Enhanced salinomycin production by adjusting the supply of polyketide extender units in *Streptomyces albus*. Metab Eng 2016;35:129–37. https://doi.org/10.1016/j.ymben.2016.02.012.

[20] Qiu J, Zhuo Y, Zhu D, Zhou X, Zhang L, Bai L, et al. Overexpression of the ABC transporter *AvtAB* increases avermectin production in *Streptomyces avermitilis*. Appl Microbiol Biotechnol 2011;92(2):337–45. https://doi.org/10.1007/s00253-011-3439-4.

[21] Zhang X, Luo H, Tao Y, Wang Y, Jiang X, Jiang H, et al. FkbN and Tcs7 are pathway-specific regulators of the FK506 biosynthetic gene cluster in *Streptomyces tsukubaensis* L19. J Ind Microbiol Biotechnol 2016;43(12):1693–703. https://doi.org/10.1007/s10295-016-1849-0.

[22] Stratigopoulos G, Gandecha AR, Cundliffe E. Regulation of tylosin production and morphological differentiation in *Streptomyces fradiae* by TylP, a deduced γ-butyrolactone receptor. Mol Microbiol 2002;45(3):735–44. https://doi.org/10.1046/j.1365-2958.2002.03044.x.

[23] Jung WS, Kim E, Yoo YJ, Ban YH, Kim EJ, Yoon YJ. Characterization and engineering of the ethylmalonyl-CoA pathway towards the improved heterologous production of polyketides in *Streptomyces venezuelae*. Appl Microbiol Biotechnol 2014;98(8):3701–13. https://doi.org/10.1007/s00253-013-5503-8.

[24] Stratigopoulos G, Cundliffe E. Inactivation of a transcriptional repressor during empirical improvement of the tylosin producer, *Streptomyces fradiae*. J Ind Microbiol Biotechnol 2002;28(4):219–24. https://doi.org/10.1038/sj/jim/7000234.

[25] Stratigopoulos G, Bate N, Cundliffe E. Positive control of tylosin biosynthesis: pivotal role of TylR. Mol Microbiol 2004;54(5):1326–34. https://doi.org/10.1111/j.1365-2958.2004.04347.x.

[26] Cho MK, Lee BT, Kim HU, Oh MK. Systems metabolic engineering of *Streptomyces venezuelae* for the enhanced production of pikromycin. Biotechnol Bioeng 2022;119(8):2250–60. https://doi.org/10.1002/bit.28114.

[27] Li D, Tian Y, Liu X, Wang W, Li Y, Tan H, et al. Reconstitution of a mini-gene cluster combined with ribosome engineering led to effective enhancement of salinomycin production in *Streptomyces albus*. Microb Biotechnol 2021;14(6):2356–68. https://doi.org/10.1111/1751-7915.13686.

[28] Wang C, Wang J, Yuan J, Jiang L, Jiang X, Yang B, et al. Generation of *Streptomyces hygroscopicus* cell factories with enhanced ascomycin production by combined elicitation and pathway-engineering strategies. Biotechnol Bioeng 2019;116(12):3382–95. https://doi.org/10.1002/bit.27158.

[29] Li L, Zhao Y, Ruan L, Yang S, Ge M, Jiang W, et al. A stepwise increase in pristinamycin II biosynthesis by *Streptomyces pristinaespiralis* through combinatorial metabolic engineering. Metab Eng 2015;29:12–25. https://doi.org/10.1016/j.ymben.2015.02.001.

[30] Hao Y, You Y, Chen Z, Li J, Liu G, Wen Y. Avermectin B1a production in *Streptomyces avermitilis* is enhanced by engineering *aveC* and precursor supply genes. Appl Microbiol Biotechnol 2022;106(5–6):2191–205. https://doi.org/10.1007/s00253-022-11854-w.

[31] Li Y, Bu Q, Li J, Xie H, Su Y, Du Y, et al. Genome-based rational engineering of *Actinoplanes deccanensis* for improving fidaxomicin production and genetic stability. Bioresour Technol 2021;330:124982. https://doi.org/10.1016/j.biortech.2021.124982.

[32] Flett F, Mersinias V, Smith CP. High efficiency intergeneric conjugal transfer of plasmid DNA from *Escherichia coli* to methyl DNA-restricting streptomycetes. FEMS

Microbiol Lett 1997;155(2):223–9. https://doi.org/10.1016/S0378-1097(97)80014-6.
[33] Kieser T, Bibb MJ, Chater KF, Butter M, Hopwood D, Bittner ML, et al. Practical *Streptomyces* genetics: a laboratory manual. Norwich: The John Innes Foundation; 2000.
[34] Zhao Y, Xiang S, Dai X, Yang K. A simplified diphenylamine colorimetric method for growth quantification. Appl Microbiol Biotechnol 2013;97(11):5069–77. https://doi.org/10.1007/s00253-013-4893-y.
[35] Livak KJ, Schmittgen TD. Analysis of relative gene expression data using real-time quantitative PCR and the $2^{-\Delta\Delta CT}$ Method. Methods 2001;25(4):402–8. https://doi.org/10.1006/meth.2001.1262.
[36] Orelle C, Mathieu K, Jault JM. Multidrug ABC transporters in bacteria. Res Microbiol 2019;170(8):381–91. https://doi.org/10.1016/j.resmic.2019.06.001.
[37] Shin SK, Xu DL, Kwon HJ, Suh JW. *S*-adenosylmethionine activates *adpA* transcription and promotes streptomycin biosynthesis in *Streptomyces griseus*. FEMS Microbiol Lett 2006;259(1):53–9. https://doi.org/10.1111/j.1574-6968.2006.00246.x.
[38] Ning X, Wang X, Wu Y, Kang Q, Bai L. Identification and engineering of post-PKS modification bottlenecks for ansamitocin P-3 titer improvement in *Actinosynnema pretiosum* subsp. *pretiosum* ATCC 31280. Biotechnol J 2017;12(11). https://doi.org/10.1002/biot.201700484.
[39] Wang Y, Wang Y, Chu J, Zhuang Y, Zhang L, Zhang S. Improved production of erythromycin A by expression of a heterologous gene encoding *S*-adenosylmethionine synthetase. Appl Microbiol Biotechnol 2007;75(4):837–42. https://doi.org/10.1007/s00253-007-0894-z.
[40] Zhang X, Fen M, Shi X, Bai L, Zhou P. Overexpression of yeast *S*-adenosylmethionine synthetase *metK* in *Streptomyces actuosus* leads to increased production of nosiheptide. Appl Microbiol Biotechnol 2008;78(6):991–5. https://doi.org/10.1007/s00253-008-1394-5.
[41] Zhao X, Wang Q, Guo W, Cai Y, Wang C, Wang S, et al. Overexpression of *metK* shows different effects on avermectin production in various *Streptomyces avermitilis* strains. World J Microbiol Biotechnol 2013;29(10):1869–75. https://doi.org/10.1007/s11274-013-1350-0.
[42] Pang A, Du L, Lin C, Qiao J, Zhao G. Co-overexpression of *lmbW* and *metK* led to increased lincomycin A production and decreased byproduct lincomycin B content in an industrial strain of *Streptomyces lincolnensis*. J Appl Microbiol 2015;119(4):1064–74. https://doi.org/10.1111/jam.12919.
[43] Liu J, Gao W, Pan Y, Liu G. Metabolic engineering of *Acremonium chrysogenum* for improving cephalosporin C production independent of methionine stimulation. Microb Cell Factories 2018;17(1):87. https://doi.org/10.1186/s12934-018-0936-5.
[44] Cai D, Zhang B, Zhu J, Xu H, Liu P, Wang Z, et al. Enhanced bacitracin production by systematically engineering *S*-Adenosylmethionine supply modules in *Bacillus licheniformis*. Front Bioeng Biotechnol 2020;8:305. https://doi.org/10.3389/fbioe.2020.00305.
[45] Zhao X, Gust B, Heide L. *S*-Adenosylmethionine (SAM) and antibiotic biosynthesis: effect of external addition of SAM and of overexpression of SAM biosynthesis genes on novobiocin production in *Streptomyces*. Arch Microbiol 2010;192(4):289–97. https://doi.org/10.1007/s00203-010-0548-x.
[46] Xu Y, Tan G, Ke M, Li J, Tang Y, Meng S, et al. Enhanced lincomycin production by co-overexpression of *metK1* and *metK2* in *Streptomyces lincolnensis*. J Ind Microbiol Biotechnol 2018;45(5):345–55. https://doi.org/10.1007/s10295-018-2029-1.
[47] Malla S, Niraula NP, Liou K, Sohng JK. Self-resistance mechanism in *Streptomyces peucetius*: overexpression of *drrA, drrB* and *drrC* for doxorubicin enhancement. Microbiol Res 2010;165(4):259–67. https://doi.org/10.1016/j.micres.2009.04.002.
[48] Wang X, Wei J, Xiao Y, Luan S, Ning X, Bai L. Efflux identification and engineering for ansamitocin P-3 production in *Actinosynnema pretiosum*. Appl Microbiol Biotechnol 2021;105(2):695–706. https://doi.org/10.1007/s00253-020-11044-6.
[49] Xia H, Li X, Li Z, Zhan X, Mao X, Li Y. The application of regulatory cascades in *Streptomyces*: yield enhancement and metabolite mining. Front Microbiol 2020;11:406. https://doi.org/10.3389/fmicb.2020.00406.